

Numerical Implementation of Helical Undulator Photon Source and Its Application in ILC Positron Source Simulation

Wanming Liu, Haitao Wang and Wei Gai

Abstract: We present a comprehensive numerical modeling of the helical undulator based positron source. In this model, we have modeled the effect of: 1)the finite length of undulator, 2)the finite distance between undulator and collimator, 3)the drive beam profile. By including these effects, this study gives a more practical picture of the ILC e^+ source parameters. We show that the inter-dependent parameters of the ILC e^+ source.

In order to produce high intensity polarized positron source for the International Linear Collider (ILC), a helical undulator based positron source scheme has been chosen as the baseline design. The front end system has been outlined by Klaus Floetman^[1], as shown in Figure 1, which includes several hundred meters of helical undulator to produce polarized γ rays, a thin titanium target (0.4X) to produce e^+ , an adiabatic matching solenoid to collect and a pre-accelerator to accelerate the positrons to about 250 MeV. Then the positrons are separated by using a separation magnet set to select the positron with matched phase space for transport into the damping ring. For a complex system such as the ILC positron source, a detailed simulation including helical undulator length effect and drive beam profile, and photon polarization and its selection by a collimator must be considered.

The radiation of helical undulator as a circularly polarized photon source for polarized positron production was first proposed by Alexander Mikhailichenko^[2] and then systematically studied by

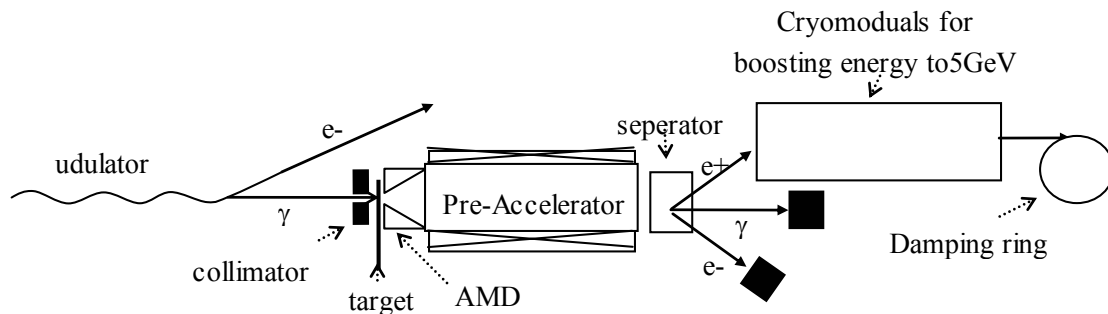


Figure 1, schematic layout of ILC polarized positron source

Klaus Floetman. The scheme has also been investigated by Yuri K. Batygin^[3] and John Sheppard^[3,4] recently. The properties of helical undulator radiation from a single electron beam have been given

analytically^[1,4] and can be directly applied to the polarized photon production for idealized cases. But in the reality, there are many practical issues need to be addressed and these practical issues are mostly not suitable for being modeled analytically. To obtain a more accurate picture of the characteristics of helical undulator radiation and the corresponding positron beam, we need to perform a systematic numerical study that incorporate many practical issues. This modeling will include the effect of the phase space distribution of drive electron beam, the effect of the length of undulator. In addition, we will also examine effect of a photon collimator and its location on the polarized positron production on the target. The yield change as a result of these practical issues will be presented and discussed.

Radiation of Helical undulator^[1,3]

For a given electron passing through a helical undulator, it travels on a spiral trajectory and produces circularly polarized radiation. The spectrum of short period helical undulator radiation was first studied by Brian M. Kincaid^[2] and the complete characteristics of this radiation is given in [1].

The important results from [1] is for a given undulator with K and first radiation harmonic energy $E_1 = \hbar\omega_1$, the radiated photon number spectrum of helical undulator can be expressed as

$$\frac{dNph}{dE} \left[\frac{1}{mMeV} \right] = \frac{10^6 e^2}{4\pi\epsilon_0 c^2 \hbar^2} \frac{K^2}{\gamma^2} \sum_1^{\infty} (J'_n(x))^2 + \left[\frac{\alpha_n}{K} - \frac{n}{x} \right]^2 J_n(x)^2 \quad (2)$$

where, n is harmonic index of the radiation and

$$\alpha_n^2 = \left[n \frac{\omega_1(1+K^2)}{\omega} - 1 - K^2 \right] \geq 0$$

$$x = 2K \frac{\omega}{\omega_1(1+K^2)} \alpha_n$$

$J_n =$ Bessel functions

From this spectrum, we can obtain the harmonic distribution function and photon energy distribution function which will be discussed in next section.

For the field amplitude of radiation, it can be obtained as

$$\begin{aligned} I_x(E) &= \sum_{n=1}^{\infty} \sqrt{\frac{10^6 e^3}{4\pi\epsilon_0 \hbar^2 c^2}} \frac{K}{\gamma} \left[\frac{\alpha_n}{K} - \frac{n}{x} \right] J_n(x) \delta(\gamma^2 \Theta^2 - \alpha_n^2) \\ I_y(E) &= i \sum_{n=1}^{\infty} \sqrt{\frac{10^6 e^3}{4\pi\epsilon_0 \hbar^2 c^2}} \frac{K}{\gamma} J'_n(x) \delta(\gamma^2 \Theta^2 - \alpha_n^2) \end{aligned} \quad (3)$$

One important feature of the above equation is for a given radiation photon frequency, the radiation from different harmonics have different radiation angle as

$$\Theta_n = \frac{1}{\gamma} \left[n \frac{\omega_1 (1 + K^2)}{\omega} - 1 - K^2 \right]^{1/2} \quad (4)$$

therefore, the radiation field from different harmonics can not be added up and then be treated as one kind of photon, even it may have the same energy. We rewrite equation (3) in terms of harmonic and energy as

$$\begin{aligned} I_x(E, n) &= \sqrt{\frac{10^6 e^3}{4\pi\epsilon_0 \hbar^2 c^2}} \frac{K}{\gamma} \left[\frac{\alpha_n}{K} - \frac{n}{x} \right] J_n(x) \\ I_y(E, n) &= i \sqrt{\frac{10^6 e^3}{4\pi\epsilon_0 \hbar^2 c^2}} \frac{K}{\gamma} J_n'(x) \end{aligned} \quad (5)$$

With the field amplitude given in (5), we can easily obtain the Stokes parameter of the undulator radiation for different harmonics and photon energies as

$$\xi_1 = \frac{I_x^2 - I_y^2}{I_x^2 + I_y^2}, \quad \xi_2 = 0, \quad \xi_3 = \frac{2I_x I_y}{I_x^2 + I_y^2} \quad (6)$$

where ξ_1 describes the linear polarization, ξ_2 describes the linear polarization in coordinate system rotated by 45° with respect to the original one for ξ_1 , ξ_3 describes the circular polarization.

The detail of the relation between polarization of photon and positron can be found in [1,2,6,7]. The detailed process on calculating the polarization of produced positrons is complicated and described in details by Klaus Floetman^[1]. In general, the final state of the produced e+ polarization is a strong function of parameter ξ_3 the photon and energy of e+. When the produced e+'s energy is close the gamma energy, then the e+ will have a polarization very closed to ξ_3 of the source photon and on contrary with much lower energy, the polarization tends to go negative values.

Photon spectrum from a distributed electron drive beam and finite length undulator

For a system layout in Figure 1, one has to consider effects of a distributed drive beam with both finite bunch length and transverse beam size. Also the distance between the undulator and the target

will be on the same order of the undulator length. In order to obtain a more accurate positron beam initial profile, we need to correlate the electron distribution into photon distribution in both transverse and longitudinal direction. And also because of the target distance is comparable to the undulator length, the undulator need to be considered as a distributed source of photon instead of a point source.

For a given photon at the target, one needs to know its' energy, direction, polarization and originating point. As being pointed out in the last section, the radiation from different harmonics can not contribute to the same photon as their radiation angle is different. The photon number spectrum needs to be decomposed in terms of harmonics in order to separate the photon from different harmonics. For the n th harmonic, its photon number spectrum can be easily extracted from equation (2) as

$$\left. \frac{dNph}{dE} \right|_n = \frac{10^6 e^2}{4\pi\epsilon_0 c^2 h^2} \frac{K^2}{\gamma^2} (J'_n(x))^2 + \left[\frac{\alpha_n}{K} - \frac{n}{x} \right]^2 J_n(x)^2 \quad (7)$$

where x is a function of the photon energy $E = \hbar\omega$ as described in equation(2)

By integrating the photon number spectrum for different harmonic, the normalized distribution function of discrete variable n , the index of radiation harmonic photon, is thus determined as

$$D(n) = \sum_{i=1}^n \int_0^\infty \left. \frac{dNph}{dE} \right|_i dE \Bigg/ \sum_{i=1}^\infty \int_0^\infty \left. \frac{dNph}{dE} \right|_i dE \quad (8)$$

After we know the originating harmonic index n of a photon, the normalized photon distribution as function of photon energy is determined by

$$D_n(E) = \int_0^E \left. \frac{dNph}{dE} \right|_n dE \Bigg/ \int_0^{E_n} \left. \frac{dNph}{dE} \right|_n dE \quad (9)$$

where E_n is the highest photon energy of the n th harmonic.

Once the photon energy and originating harmonic is determined from equation (8) and (9), the polarization and radiation angle is also determined. However, the originating point of the photon also needs to be given. Here we assume that the helical field is uniform transverse across the of drive electron beam. The longitudinal and transverse distributions of electron will be correlated into photon distributions at the originating location. In the numerical implementation, the longitudinal coordinate of photon's originating point will be assigned randomly along the length of undulator. In our implementation, the electron beam is assumed to have standard Gaussian distribution in both longitudinal and transverse direction. Given the σ of longitudinal and transverse distributions drive electron beam, we can then determine properties of the photon distribution based on the emitting electron distribution and their originating points in the undulator.

Once the distribution is uniquely determined, one needs to consider the polarizations of each individual photon at the target. From references [1, 2, 4, 5], the polarization of helical undulator

radiation is depending on the emitting angle of radiation. The smaller the angle, the more circularly the polarization is. In order to maximize the polarized e⁺ yields, one need to ensure the photons has maximum circular polarizations. This will require implementation of a small aperture before the target to collimate the photon distribution so only the small angle photons are allowed to strike on the target.

In our study, the collimator will be represented as an iris at a certain distance away from the end of undulator on the axis of beam line. The iris radius and its location together will setup a filter on the radiation of helical undulator. Changing these two parameters of collimator, the positron yield and polarization will change.

To implement the collimator numerically, given the photon a direction vector as (dx,dy,dz), which is determined by photon energy and index of originating harmonic, and a originating point as (x₀,y₀,z₀), which is determined by drive beam parameters, its status after the collimator will be determined by the position at where it hits the collimator screen

$$r = \sqrt{[x_0 + (z_c - z_0)dx / dz]^2 + [y_0 + (z_c - z_0)dy / dz]^2} \quad (13)$$

where z_c is location of collimator. If r is smaller than the iris radius of collimator, the photon is alive after the collimator, otherwise it will be killed.

Up to this point, we have established the photon generating and selecting procedures. Following these procedures, we can produce photons with given undulator parameters, electron beam parameters and collimator settings. Using these photons as input for the EGS^[8] simulations, we can then obtain the positron beam distribution at the exit of target surface. Then by using the obtained positron beam distribution as initial particle distribution, we can set up the positron beam dynamic simulation and track the positron beam to the entrance of damping ring using PARMELA^[9].

Application to ILC Positron Source Simulation

There are two important criteria for the ILC positron source: yields and polarization. The positron yield rate is calculated by the ratio of number of positrons accepted by the damping ring over the number of electron going through the helical undulator. Polarization of beam is obtained from the polarization of positrons before injected into the damping ring. ILC polarized positron source required a polarization >60% and yield of 1.5. For its base line parameter, the ILC helical undulator parameter is K=1 and B=1.07T. All the simulations presented here are based on this undulator parameter.

Before we start applying this implementation, we would like to confirm its effectiveness first. By the results showing in figure 2, we confirmed that the practical issues like drive beam profile, finite undulator length and drift between collimator and undulator are very important when dealing with the reality. As showing in figure 2, we compared three cases: 1) the point source model where the photons from undulator with temporal profile of drive beam; 2) point source with temporal and transverse profile of drive beam which moves it one small step towards the reality.; 3) our model with

finite length of undulator, finite distance between collimator and undulator and drive beam phase space profile. The collimator cutting angle is the same at $3.85\mu\text{rad}$ for all 3 cases. The drive beam is assumed to have $\sigma_t=1.5\text{ps}$ and $\sigma_x=\sigma_y=100\mu\text{m}$. As shown in the figure, with and without considering the drive beam transverse profile can make significant difference. For the same collimator acceptance angle, when treated the undulator as a point source, case 1), the yield decreases monotonously and the polarization is about constant while increasing the drift between collimator and undulator. But for case 2, the yield curve and polarization curve behaves quite differently. And for case 3, which is the most closed to the real undulator radiation, the result is completely different from the other 2 cases. As one can expect from this figure, these 3 sets of curves will definitely converge when the drift is long enough. But when the drift is only few hundreds meters, which is comparable to the length of undulator, the effects of distributed sources are very important and should be treated properly.

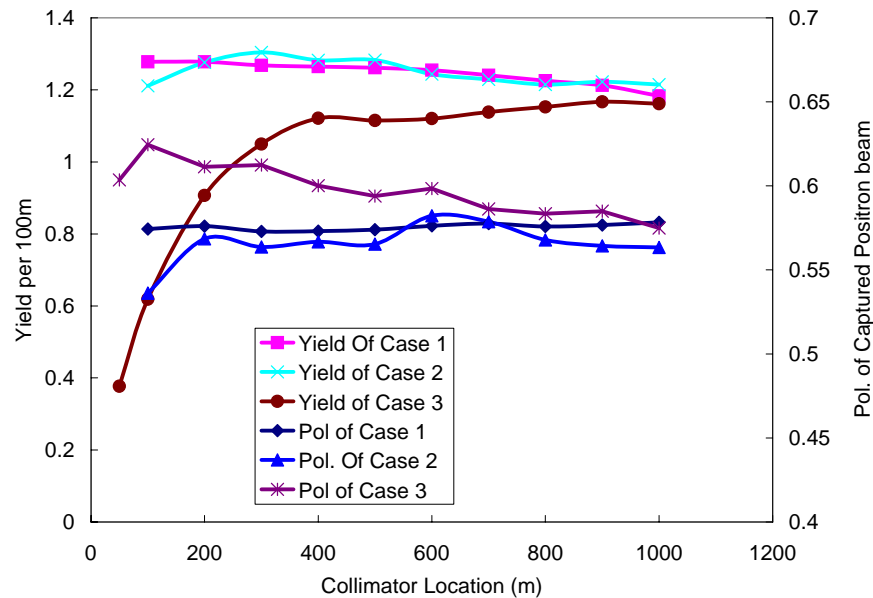


Figure 2. Comparing of results from 1) model of point source + temporal profile of drive beam; 2) model of point source + temporal and transverse profile of the drive beam; and 3) our model. In all three cases comparing here, the half angle of collimator acceptance cone, as referenced to the end of undulator, is fixed as $3.85\mu\text{rad}$.

In figure 3, the results of collimators with a fixed location at 700m are given. The length of undulator is assumed to be 100m when generating photons in EGS simulation. As shown in the figure, the yield increases while the polarization decreases. The optimum yield for this configuration would be about 1.07 positrons per electron per 100m undulator where the polarization crossing 60%.

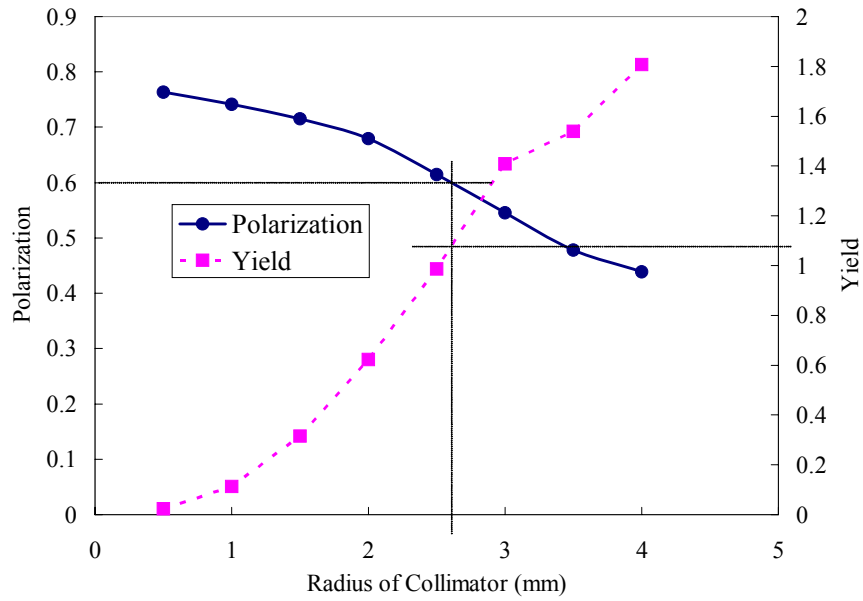


Figure 3. Polarization and Yield results of collimators with fixed location at 700m. The radius of collimator varies from 0.5mm to 4mm.

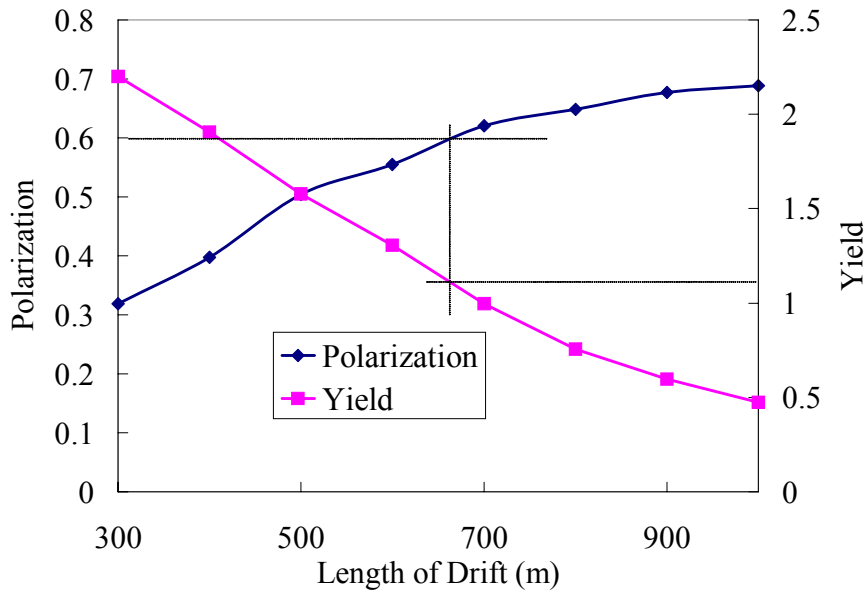


Figure 4. Polarization and yield results of using collimator with fixed iris radius at 2.5mm. The distance between the end of undulator and collimator is changing from 300m to 1000m.

In figure 4, we give the results of positron yield and polarization for a set of fixed iris collimators. The radius of the collimator is fixed at 2.5mm, the target is immediately following the collimator, and thus the hard edge radius of the photon spot on target is also fixed at 2.5mm. By doing this, the effect of changing photon spot size on target could be ignored in interpreting the data. As showing in the figure, the yield is decreasing when increasing the length of drift while the polarization is increasing with the increasing of the drift length. The optimum drift length for a 2.5mm collimator would be 660m where the polarization just satisfying the ILC requirement. The optimum yield for collimators with iris radius at 2.5mm is about 1.1 positrons per electron and 100 meters.

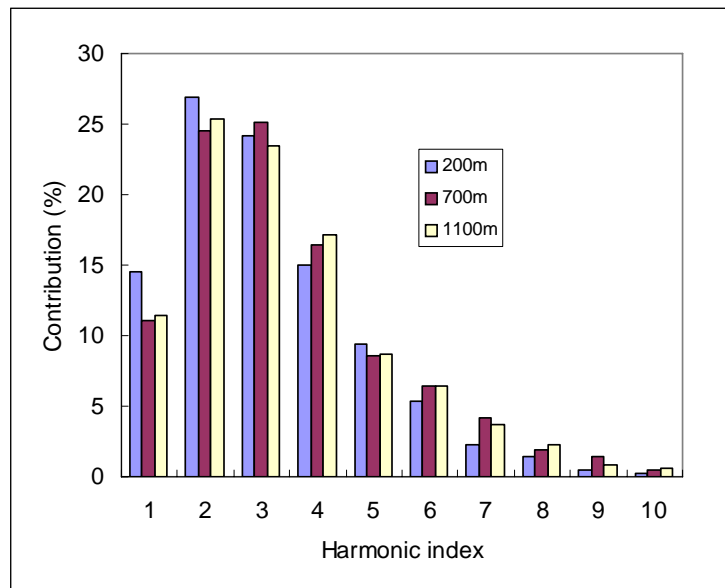


Figure 5, Contribution of harmonics to the positron yield. The collimator has a fixed acceptance half angle about $3.85\mu\text{rad}$. Target is located right after the collimator. Same drive electron beam parameters were used for all these 3 cases.

In figure 5, the yield distribution among harmonics of undulator radiation is given. The length of undulator is assumed to be 100m. The cutting angle of collimator is about $3.85\mu\text{rad}$ as reference to the end point of undulator. The drift between collimator and the end point of undulator were 200m, 700m and 1100m. As showing in the figure, the 1st harmonic only contribute $<15\%$ to e^+ yield. The 2nd and 3rd harmonics together contribute $>45\%$ of the yield. The 4th and 5th harmonics has contribution comparable to the 1st harmonic.

Showing in figure 6 is a plot of the initial polarization vs energy of captured positrons of the optimum collimator setting for cutting angle of $3.85\mu\text{rad}$. As showing in the figure, we can see that the positrons produced by the photons from 1st harmonic have the highest average polarization. But as showing in figure 4, these positrons only consist less than 15% of captured positron beam. Most of the captured positrons are produced by photons from 2nd, 3rd, 4th and 5th harmonics.

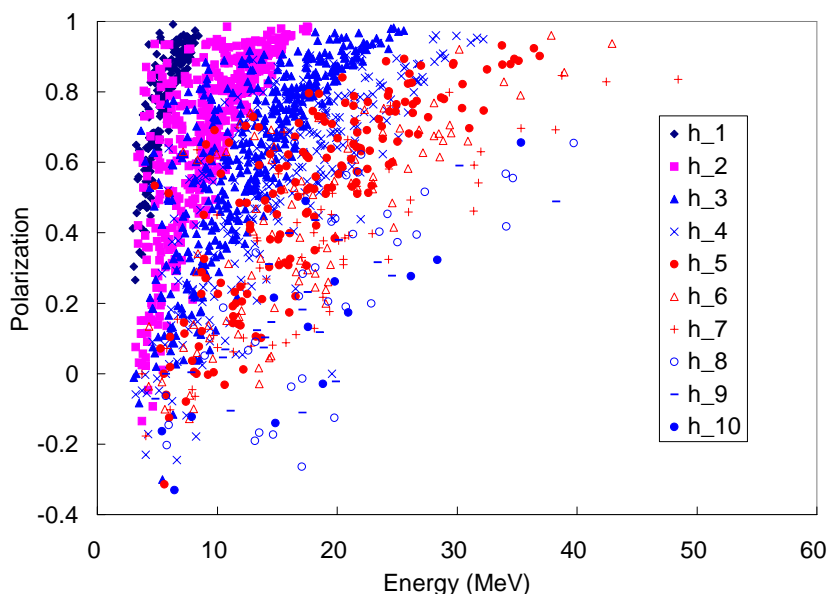


Figure 6. Plot of initial polarization vs energy of captured positrons grouped by the harmonic index of the photon.

Summary

A numerical implementation of helical undulator photon source with practical considerations is developed and discussed in this paper. As the numerical simulation results showing, this numerical implementation, with many practical issues addressed, is very important and necessary for predicting the performance of ILC polarized positron sources. Using this numerical implementation of helical undulator photon source, we also revealed some interesting facts for the first time. As shown in the results, it is the photons from higher order harmonics which produced most of the positrons. The 1st harmonic makes less than 15% of the yield. The higher order harmonics contributed more than 85% to the yield.

Reference

- [1] Klaus Flottmann, Investigation toward the development of polarized and unpolarized high intensity positron sources for linear colliders, DESY 93-161
- [2] V. Balakin, A. Mikhailichenko, Conversion system for obtaining highly polarized electrons and positrons at high energy, Budker INP 79-85, September 13, 1979
- [3] Y.K. Batygin and J.C. Sheppard, Post-target beamline design for proposed FFTB experiment with polarized positrons, Linear Collider Collaboration Tech Note, lcc-0110, December 2002
- [4] J. C. Sheppard, Helical Undulator Radiation, Linear Collider Collaboration Tech Note, lcc-0095, July 2002

- [5] B. M. Kincaid, A short-period helical wiggler as an improved source of synchrotron radiation, *Journal of Applied Physics*, Vol. 48; No 7(1977) 2684-2691
- [6] H. Olsen, L.C. Maximon, Photon and Electron Polarization in Bremsstrahlung and Pair Production with Screening, *Physical Review*, 114, 887, (1959)
- [7] H. Olsen, L.C. Maximon, Electron and Photon Polarization in Bremsstrahlung and Pair Production, *Physical Review*, 110, 589, (1958)
- [8] I. Kawrakow and D.W.O. Rogers, The EGSnrc Code System: Monte Carlo Simulation of Electron and Photon Transport, NRCC Report *PIRS-701*
- [9] Lloyd M. Young, and James H. Billen, "PARMELA", LA-UR-96-1835, Revised April 28, 2004.